Reprint 509

LIDAR Observations of Terrain-induced Flow and its Application in Airport Wind Shear Monitoring

C.M. Shun, C.M. Cheng & O.S.M. Lee

International Conference on Alpine Meteorology (ICAM)
and Mesoscale Alpine Programme (MAP) Meeting,
Brig, Switzerland, 19-23 May 2003

LIDAR Observations of Terrain-induced Flow and Its Application in Airport Wind Shear Monitoring

C.M. Shun, C.M. Cheng and O. Lee

Hong Kong Observatory, Hong Kong

1. Introduction

Hong Kong installed a Doppler LIght Detection And Ranging (LIDAR) System at the Hong Kong International Airport (HKIA) in mid-2002 to detect wind shear under clear-air conditions. The LIDAR is the first of its kind in the world for operational airport weather alerting.

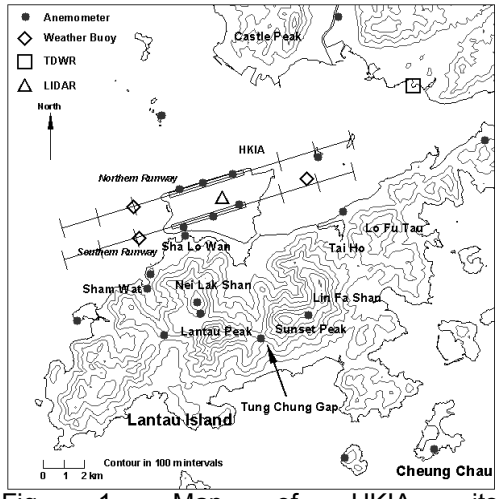

Fig. 1. Map of HKIA, its approach/departure corridors and surrounding areas. Terrain contours are given in 100 m intervals.

In aviation, wind shear is a sustained change (i.e. lasting more than a few seconds) in headwind, resulting in a change in the aircraft lift. A change of 15 kt (7.7 ms^{-1}) or more in headwind or tailwind is considered significant wind shear requiring corrective action by the pilot. Reports of wind shear received from aircraft landing at or taking off from HKIA since its opening in 1998 indicated that low-level wind shear could occur in rainy weather as well as in clear-air conditions. A majority of the clear-air events were associated with disturbed airflow reaching the airport after passing over the hilly terrain of Lantau Island – a mountainous island south of the airport, with peaks up to around 1 000 m. Figure 1 illustrates the complex terrain of Lantau and the location of HKIA and its approach/departure corridors relative to this terrain. Since early 1997, a Terminal Doppler Weather Radar (TDWR) has been used to monitor the wind flow around HKIA. During passages of tropical cyclone, it captured features in the air flow revealing the presence of high- and low-speed streaks, re-circulation vortices, periodic vortex shedding and gap-related downslope flow on the lee of Lantau Island (Shun and Lau, 2000). The newly installed pulsed Doppler LIDAR, operating at 2 micron wavelength, supplements the TDWR in monitoring the wind flow around HKIA in rain-free weather. Shun and Lau (2002) provided a detailed description of the LIDAR implementation. See Figure 1 for location of the LIDAR and TDWR.

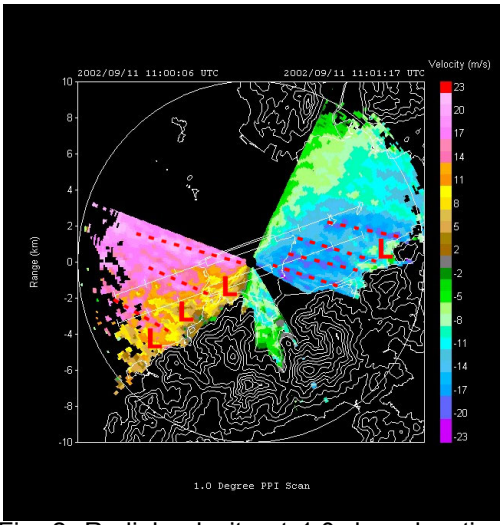

Fig. 2. Radial velocity at 1.0 deg elevation at 11:00 UTC on 11 Sep 2002 (dotted lines indicating high-speed streaks and 'L' indicating low-speed streaks in between).

Since its installation in mid-2002, the LIDAR has observed interesting terrain-induced phenomena downwind of Lantau, including disrupted flow during the passage of a tropical cyclone, cases of apparent hydraulic jump, and downslope flow from mountain gaps. These LIDAR observations are presented below.

2. Terrain-induced Flow in Tropical Cyclone

On windy occasions such as the passage of a tropical cyclone, streaks of high wind speed were observed to emerge from valleys of Lantau. Lying between these high-speed air streaks are lower speed air streaks downwind of peaks. Aircraft traversing these alternating high-speed and low-speed air streaks would encounter alternating headwind losses and gains along the approach and departure paths. Figure 2 shows such a situation as observed by the LIDAR during the passage of Severe Tropical Storm Hagupit on 11 September 2002, when HKIA was affected by strong ESE'ly winds.

3. Downslope Flow and Hydraulic Jump

Based on water tank studies using a physical model of Lantau, Baines and Manins (1989) simulated the existence of hydraulic jumps downwind of Lantau in SW through E'ly winds when low-level temperature inversion was present. Before the installation of the LIDAR, little evidence was available to ascertain the presence of hydraulic jump over Lantau. Chan and Tam (1996) referred to the presence of Foehn effect in respect of higher temperatures at Sha Lo Wan (SLW) relative to Cheung Chau (see Figure 1 for their locations) in SE'ly flow. Lau and Shun (2000) also noted an updraft reaching 3 ms^{-1} as measured by a wind profiler at SLW under a strong E'ly flow.

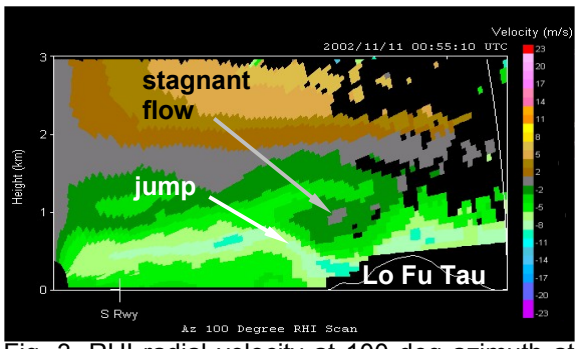

Fig. 3. RHI radial velocity at 100 deg azimuth at 00:55 UTC on 11 Nov 2002.

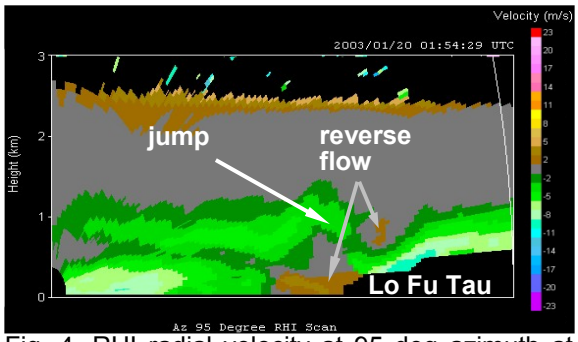

Fig. 4. RHI radial velocity at 95 deg azimuth at 01:54 UTC on 20 Jan 2003.

The first LIDAR observation (Figure 3) of a jump like feature was noted in the morning of 11 November 2002 on a Range Height Indicator (RHI) scan pointing at 100 degrees, i.e. towards a hill named Lo Fu Tau (465 m, see Figure 1) when the upstream flow was ESE with flow speed (U_0) ~ 5 ms^{-1}. The jump-like feature consisted of: (a) downslope flow with radial winds of up to about −10 ms^{-1} (i.e. towards the LIDAR) almost reaching the ground; (b) an elevated low-level jet connecting to the downslope flow further downwind; and (c) a stagnant flow region above the downslope flow. While the lower atmosphere was stably stratified with a Brunt-Väisälä frequency (N) of 0.0135 s^{-1} (from the radiosonde ascent at 00 UTC (local time = UTC + 8 h) at King's Park (KP), about 25 km east of HKIA), only a very weak inversion was present (0.4 °C) below 500 m. The value of Nh/ U_0 is estimated at 1.3, consistent with the value $Nh/U_0 > 0.85$ obtained by Huppert and Miles (1969) for wave breaking.

Another jump-like feature was observed on the LIDAR RHI scan on 20 January 2003 downwind of Lo Fu Tau (Figure 4). Here the downslope flow did not quite reach the ground but reverse flow can be seen above the jump and below it. The lower reverse flow region can be clearly seen in the 1.0 degree elevation LIDAR scan in Figure 5. Smaller pockets of reverse flow were also observed, being shed downwind from this region in the subsequent LIDAR scans (not shown). From the KP radiosonde ascent at 00 UTC, two closely spaced temperature inversions of 1.1 °C and 1.5 °C were present between 500 and 700 m, producing a change in the potential temperature ($\Delta\theta$) of 3.6 K. Taking N ~ 0.013 s^{-1} (average value below 600 m), we obtain Nh/U_0 ~ 1.0, again greater than the 0.85 threshold for wave breaking. Also, with a significant inversion layer in this case, it is possible to estimate the Froude number (Fr) = $U_0/(g'D)^{½}$ at 0.7 taking U_0 ~ 6 ms^{-1}, $g' = g\Delta\theta/\theta$ = 0.12 ms^{-2} with θ = 291 K, and D ~ 600 m. Together with the dimensionless mountain height M = h/D ~ 0.8, this Fr value falls into Regime IIb of Schär and Smith (1993), viz. wake regime associated with the formation of a hydraulic jump including reverse flows in the wake.

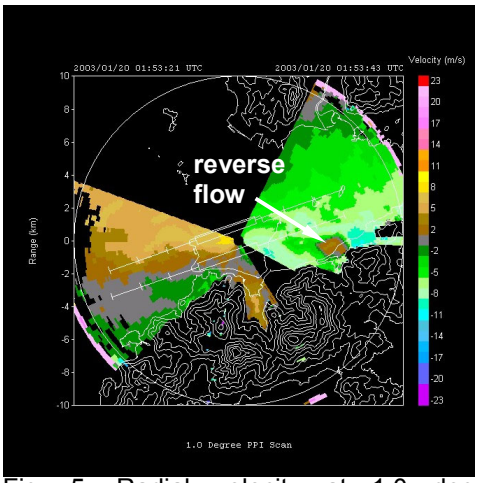

Fig. 5. Radial velocity at 1.0 deg elevation at 01:54 UTC on 20 Jan 2003.

4. Springtime Wind Shear

Aircraft reports of wind shear over the past few years indicate that spring is the peak season of terrain-induced wind shear at HKIA. Based on TDWR and aircraft observations, Lau and Shun (2000) concluded that in a stably stratified easterly flow with N ~ 0.014 s^{-1} and Nh/ U_0 in the range 1.05-1.26, mountain wake with reverse flows were present on the lee of Lantau, bringing wind shear to aircraft on approach to HKIA. With the installation of the LIDAR and additional anemometers on weather buoys (see Figure 1), we are now able to better understand the complex flow leading to such phenomena.

On 5 March 2003, HKIA was affected by strong easterly flow which veered rapidly with height to the south, reaching gale force on hilltop of Lantau. 26 wind shear reports with headwind changes of 15 kt (7.7 ms^{-1}) or more were received, four of them reaching 30 kt (15.4 ms^{-1}). At 00 UTC, the KP radiosonde ascent indicated the presence of a low-level SE'ly jet with maximum speed of 19 ms^{-1} near 750 m and a sharp temperature inversion of 3.7 °C between 400 and 600 m. Figure 6 shows the LIDAR Doppler radial velocity at 1.0 degree elevation at 03:17 UTC, just 1 minute after an aircraft reported a 30 kt wind shear on approach to the northern runway from the west. It shows a pattern quite different from that shown in Figure 2 when HKIA was affected by strong ESE'ly flow associated with a tropical cyclone. Specifically, Figure 6 reveals several jets, oriented in different directions, downwind of Lantau (labelled as J1-J5), with J2-J5 apparently emerging from mountain gaps. While J2 may not be obvious in Figure 6 due to its southerly direction being almost tangential to the LIDAR beams, its presence is corroborated by surface wind observation at around the same time (Figure 7).

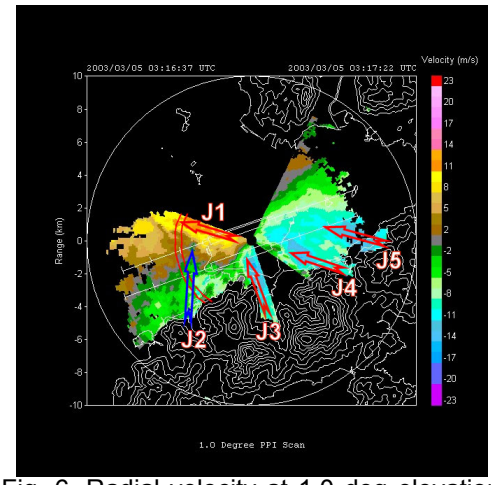

Fig. 6. Radial velocity at 1.0 deg elevation at 03:17 UTC on 5 Mar 2003 (arc indicating the range of data presented in Fig. 8).

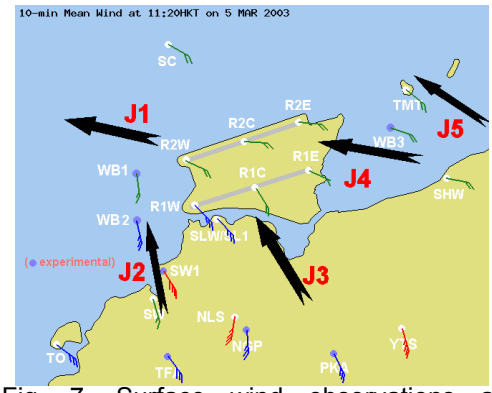

Fig. 7. Surface wind observations at 03:20 UTC on 5 Mar 2003.

Examination of surface measurements at WB1 (see Figure 7 for location) revealed a jump in the temperature from 20 °C (which was close to the measured sea surface temperature at WB1) to 24 °C once the wind turned from ENE to SSE between 01:30 and 01:40 UTC. Similar changes were observed earlier at two nearby stations: (a) a change in the temperature from 20 °C to 25 °C at WB2 as the wind turned from E to SSE between 01:00 and 01:10 UTC; and (b) an increase in the SE'ly winds at SW1 from 4 ms^{-1} to almost 20 ms^{-1} between 00:40 and 01:00 UTC. All these changes strongly suggest that J2 was a result of downslope flow over Lantau (most probably through the gap above the valley of Sham Wat (see Figure 1)), bringing a southerly air mass with high potential temperature (θ ~ 297 K) from aloft. From the KP radiosonde ascent at 00 UTC, such potential temperature corresponded to a height of 600 m or above. As similar temperature increases were also noted at SLW and over HKIA but not at WB3, it appeared that J3 was also a manifestation of downslope flow. Based on the KP radiosonde ascent at 00 UTC, if we take N ~ 0.02 s^{-1} (average value below 1 000 m), h ~ 934 m (height of Lantau Peak, see Figure 1), we obtain $Nh/U_0 \geq 1$ since $U_0 \leq 19$ ms^{-1}. This is consistent with the result of Hunt and Snyder (1980) in which a descending flow and even a hydraulic jump can be expected downwind of a model hill for $Nh/U_0 \geq 1$ and $Nh/U_0 >> 1$ respectively.

It is apparent that the wind shear event over the approach to the northern runway around the time of Figures 6 and 7 was a result of the interactions between J2 and J1. To illustrate the temporal variations of these interactions, we plot a Hovmüller diagram (azimuth versus time) of the LIDAR radial velocity at 1.0 degree elevation at a fixed range (with 3-gate averaging) which cuts across the locations of WB1 and

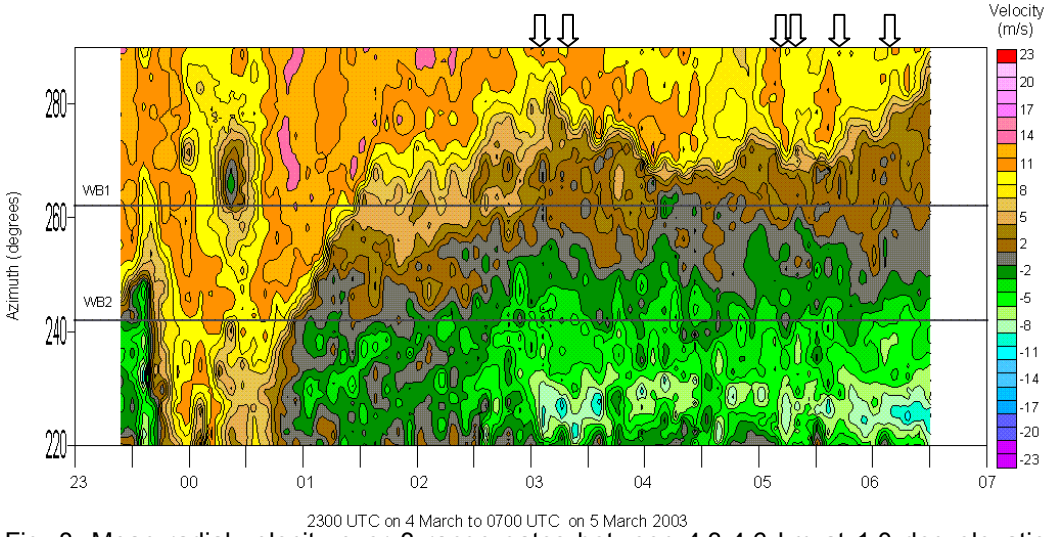

Fig. 8. Mean radial velocity over 3 range gates between 4.3-4.6 km at 1.0 deg elevation ("cool" colours indicate -ve velocities; arrows indicate time of aircraft reports of wind shear).

WB2 (Figure 8). The onset of the downslope flow J2 (-ve radial velocities, shaded) was concurrent with the northward shift (i.e. increase in azimuthal location) of the easterly flow associated with J1 (+ve radial velocities) between 00:40 and 01:40 UTC. Thereafter the interface between J2 and J1 (signified by near-zero radial velocities) remained close to the WB1 location with large radial velocity gradient appearing just to the north of WB1 between 03 and 04 UTC and also after 05 UTC. Within these periods, six aircraft reports of wind shear (time of occurrence indicated in Figure 8) were received.

To summarize, in a strongly stably stratified atmosphere with surface easterly flow veering rapidly with height to the south, the strong S'ly winds aloft were able to descend to the surface near Sham Wat after crossing Lantau, bringing about a surface S'ly jet (J2) which interacted with the surface easterly flow (J1) over the airport approaches. However, as J2 (and J3 as well) appeared to have emerged from mountain gaps, further analysis will be required to understand the extent of contribution of the "gap-flow" mechanism to the formation of these jets.

LITERATURE

Baines, P.G. and P.C. Manins, 1989: The principles of laboratory modeling of stratified atmospheric flows over complex terrain. J. Appl. Meteor., **28**, 1213-1225.

Chan, P.W. and C.M. Tam, 1996: Trapped lee waves over Lantau Island: case studies. HKMetS Bulletin Vol. 6, No. 2, 41-55.

Hubert, H.E. and J.W. Miles, 1969: Lee waves in stratified flow. Part 3: semi-elliptical obstacles. *J. Fluid Mech.*, **35**, 481-496.

Hunt, J.C. and W.H. Snyder, 1980: Experiments on stably and neutrally stratified flow over a model three-dimensional hill, *J. Fluid Mech.*, **96**, 671-704.

Lau, S.Y. and C.M. Shun, 2000: Observation of terrain-induced windshear around Hong Kong International Airport under stably stratified conditions, *9th AMS Conf. on Mountain Meteorology*, 93-98.

Schär, C. and R.B. Smith, 1993: Shallow-water flow past isolated topography. Part I: vorticity production and wake formation. *J. Atmos. Sci.*, **50**, 1373-1400.

Shun, C.M. and S.Y. Lau, 2000: Terminal Doppler Weather Radar (TDWR) observation of atmospheric flow over complex terrain during tropical cyclone passages. *SPIE Microwave Remote Sensing of the Atmosphere and Environment II*, October 2000.

Shun, C.M. and S.Y. Lau, 2002: Implementation of a Doppler Light Detection And Ranging (LIDAR) system for the Hong Kong International Airport, *Preprints, 10th AMS Conf. on Aviation, Range and Aerospace Meteorology,* 255-256.